Comparison and Evaluation of Different MODIS Aerosol Optical Depth Products Over the Beijing-Tianjin-Hebei Region in China

Jing Wei and Lin Sun

***Abstract*—Many aerosol retrieval algorithms based on the remote sensing technology have been developed and applied to produce aerosol optical depth (AOD) products for different satellite sensors. The dark target (DT) and deep blue (DB) algorithms are two main MODIS aerosol retrieval algorithms that are suitable for dark or bright areas. The estimation of land surface reflectance (LSR) is necessary to improve the accuracy of AOD retrievals. Therefore, in this paper, a new procedure to improve LSR estimation using MODIS surface reflectance products is developed. A new high-resolution <1000 m> aerosol retrieval algorithm with *a priori* LSR database support (HARLS) is proposed. The purpose of this paper is to evaluate the spatial adaptability of different MODIS AOD products produced by the above three algorithms. The Beijing-Tianjin-Hebei (Jing-Jin-Ji) region, which features complex surface structures and serious air pollution, was chosen as the study area, and the different AOD products are validated using aerosol robotic network (AERONET) AOD ground measurements from four stations located in dark and bright areas. Compared with the DT retrievals ($R \approx 0.88 - 0.95$), the C6 DB AOD retrievals yield a stronger correlation ($R \approx 0.94 - 0.97$) with AERONET AOD and lower RMSE, MRE and MAE values, resulting in approximately 20%–30% less average overestimation. The C6 DT&DB AOD results show a retrieval quality ($R \approx 0.93 - 0.97$) similar to that of DB, with approximately 50%–70% of the collections falling within the expected error (EE). Moreover, DT&DB is much better than DT, with more than approximately 10%–20% of the collections falling within the EE. However, HARLS achieves a high correlation ($R \approx 0.93 - 0.96$) with the AERONET AODs, with low RMSE ($\approx 0.118 - 0.128$) and MAE ($\approx 0.09 - 0.12$) and small offsets (intercept $\approx 0.00 - 0.04$). HARLS retrievals exhibited 7%–8% less uncertainty than the C6 DB retrievals, 37%–38% less uncertainty than the C6 DT&DB retrievals, and 39%–44% less uncertainty than the C5 and C6 DT retrievals. HARLS achieves greater accuracy and reliability in AOD retrieval, and it is less biased (RMB $\approx 0.90 - 1.10$) and better overall than the routine MODIS aerosol products over the Jing-Jin-Ji region.**

***Index Terms*—Aerosol optical depth (AOD), Beijing-Tianjin-Hebei, dark target (DT), deep blue (DB), moderate resolution imaging spectroradiometer (MODIS), high-resolution aerosol retrieval algorithm with a prior LSR database support (HARLS).**

Manuscript received May 19, 2016; revised June 25, 2016 and July 23, 2016; accepted July 26, 2016. Date of publication September 1, 2016; date of current version February 13, 2017. This work was supported in part by the National Natural Science Foundation of China [41171270], in part by the Outstanding Youth Foundation of Shandong Province [JQ201211], and in part by the Graduate Innovation Foundation of Shandong University of Science and Technology [YC150103]. *(Corresponding author: Lin Sun.)*

The authors are with the Geomatics College, Shandong University of Science and Technology, Qingdao, China (e-mail: weijing_rs@163.com; sunlin6@126.com).

Color versions of one or more of the figures in this paper are available online at http://ieeexplore.ieee.org.

Digital Object Identifier 10.1109/JSTARS.2016.2595624

I. Introduction

ATMOSPHERIC aerosols are composed of solid, liquid, and gaseous particles suspended in the atmosphere, and their diameters range from 10^{-3} to 10^{2} μm. Aerosol particles cause warming or cooling effects through direct radiation force by absorbing and scattering solar radiation. As a result, aerosol particles have important influences on local and global ecological environments and climate change [1]–[4]. Atmospheric aerosol is also the primary pollutant affecting atmospheric environmental quality. This pollutant causes degradation of visibility and increases in $PM_{2.5}$ and PM_{10}, and it presents a hazard to human health through the distribution of harmful substances [5]–[9]. Therefore, a full understanding of the impacts of aerosol particles on climate change and air quality is of important practical significance and requires the retrieval of aerosol and evaluation of its characteristics.

Satellite remote sensing is an effective means for aerosol monitoring, and aerosol optical depth (AOD) is the main parameter that can be obtained using remote sensing. The basic principle of AOD retrieval is to distinguish surface reflectance and the reflectance at the top of atmosphere (TOA) from the total satellite signals. Because land presents more complex surface structures and greater difficulties with surface reflectance estimation, AOD retrieval over land is relatively difficult. Researchers have developed various techniques to retrieve AOD over land using different satellite sensors, including moderate resolution imaging spectroradiometer (MODIS) [10]–[11], total ozone mapping spectroradiometer [12], ozone monitoring instrument [13], advanced very high-resolution radiometer [14], multiangle imaging spectro radiometer [15], SeaWiFS (sea—viewing wide field of view sensor) [16], visible infrared imaging radiometer suite [17], [18], Landsat 8 OLI (operational land imager) [19], and HJ-1 CCD (charge-coupled device sensor) [20].

The Terra and Aqua satellites were successfully launched in December 1999 and May 2002, respectively, and were each equipped with a MODIS sensor. MODIS has 36 spectral bands that span the wavelengths from visible to thermal infrared (0.41 to 14 μm) at moderate spatial resolutions (250, 500, and 1000 m) with a temporal resolution of 1 to 2 days. Due to its moderate spatial resolution, wide wavelength coverage, and short revisiting period, MODIS has been widely used for monitoring aerosol properties, and it provides long time series of global aerosol products at different resolutions. Several MODIS aerosol retrieval algorithms have been developed. Among these

algorithms, the dark target (DT) algorithm [10]–[11], [21] was the first and most popular one used to retrieve AOD from MODIS data. National Aeronautics and Space Administration (NASA) produced and provided early daily aerosol products (MOD04) based on this algorithm. However, the DT algorithm is limited to retrieving AOD over dense vegetation areas and is ineffective over bright surfaces. Subsequently, the deep blue (DB) algorithm [22]–[24] was proposed to retrieve AOD over surfaces with much higher reflectance than that of dense vegetation areas, and it was used to produce AOD products in later versions of the MODIS product suite, Collection 5.1 (C5) and Collection 6 (C6). The spatial resolutions of MOD04 DT and DB AOD products are 10 or 3 km. Therefore, to improve the spatial resolution of AOD retrieval from MODIS data, the high-resolution <1000 m> aerosol retrieval algorithm with a priori land surface reflectance (LSR) database support (HARLS) is proposed in this paper.

This study aims to evaluate the AOD precision obtained using the three algorithms. Long time-series data of MOD04 C5 and C6 DT AOD (10 km), C6 DB AOD (10 km), C6 DT&DB AOD (10 km), and HARLS AOD (1000 m) from 2013 to 2014 were obtained for this purpose. To clearly understand the regional adaptability of each method, the Beijing-Tianjin-Hebei (Jing-Jin-Ji) region, which features complex land structures and serious air pollution, was chosen as the study area, and the corresponding aerosol robotic network (AERONET) observation data were obtained for validation purposes.

II. MODIS Aerosol Retrieval Algorithms Over Land

The TOA reflectance received by satellite can be defined as a function of the atmospheric path reflectance and surface reflectance function. The TOA reflectance is a function of the solar and view zeniths and azimuth angles and can be estimated as follows [25], [26]:

$$\rho^{*}\ (\theta_s, \theta_v, \varphi) = \rho_{\mathrm{Ray}}\ (\theta_s, \theta_v, \varphi) + \rho_{\mathrm{Aer}}\,(\theta_s, \theta_v, \varphi) + \frac{\rho_s}{1-\rho_s S} T\,(\theta_s)\,T\,(\theta_v) \quad (1)$$

where $\rho^{*}(\theta_s, \theta_v, \varphi)$ is the TOA reflectance; $\rho_{\mathrm{Ray}}(\theta_s, \theta_v, \varphi)$ is the Rayleigh reflectance resulting from multiple scattering in the absence of aerosols; $\rho_{\mathrm{Aer}}(\theta_s, \theta_v, \varphi)$ is the aerosol reflectance resulting from multiple scattering in the absence of molecules; ρ_s is the surface reflectance; S is the atmospheric backscattering ratio; $T(\theta_s)$ is the transmission of the atmosphere along the sun-surface path; $T(\theta_v)$ is the transmission of the atmosphere along the surface-sensor path; and θ_s, θ_v, and φ are the solar zenith angle, view zenith angle, and relative azimuth angle, respectively.

According to (1), the signals obtained by the satellite sensor include three parts: the aerosol reflectance, the Rayleigh reflectance, and the reflectance contributed by surface and atmospheric interaction. Rayleigh scattering is an extensive factor and has a significant impact on the visible channels, especially the blue bands (412–490 nm) with short wavelengths. Therefore, it needs to be eliminated first.

The Rayleigh scattering correction for satellite data depends on the determination of the Rayleigh phase function and the Rayleigh optical Depth (ROD) [27]–[29]. In this paper, the three AOD retrieval algorithms select the same Rayleigh scattering correction method, which was proposed by Bodhaine *et al*. [30] and is represented by the following equation:

$$\tau_{\mathrm{Ray}}\ (\lambda, \mathrm{z}=0) = -0.00877\ \lambda^{-4.05} \quad (2)$$

where τ_{Ray} is the ROD, λ is the wavelength (μm), and z is the ground elevation (height) above sea level in kilometers (km).

The ROD can be expressed as a function of atmospheric pressure (or height, z) [31] and can be corrected using the height data from the MOD03 geolocation product:

$$\tau_{\mathrm{Ray}}\ (\lambda, \mathrm{z}=\mathrm{Z}) = \tau_{\mathrm{Ray}}\ (\lambda, \mathrm{z}=0) \exp\left(\frac{-\mathrm{Z}}{8.5}\right) \quad (3)$$

where Z is the height (km) of the surface target and 8.5 km is the exponential scale height of the atmosphere. AOD information is located in the last two parts of (1); to retrieve AOD from these parts, the surface reflectance should be estimated first. The three methods differ in how AOD is retrieved and are introduced in the following sections.

A. MODIS DT Aerosol Retrieval Algorithm Over Land

The MODIS DT algorithm contains two entirely independent algorithms, one for aerosol retrieval over land and the second for aerosol retrieval over ocean. The DT algorithm was first proposed by Kaufman *et al.* based on the finding that the surface reflectance over dark surfaces was low in the blue and red channels and showed a nearly fixed ratio, with the TOA reflectance at 2.13 μm ($\rho^{*}{}_{2.13}$). As such, the surface reflectance at the red ($\rho_{0.66}$) and blue ($\rho_{0.46}$) bands can be estimated using the TOA reflectance at 2.13 μm ($\rho^{*}{}_{2.13}$) via empirical relationships ($\rho_{0.46} = 0.25\rho^{*}{}_{2.13}$; $\rho_{0.66} = 0.5\rho^{*}{}_{2.13}$) [10], [11]. Pixels with TOA reflectance in the range of 0.01–0.25 in the 2.13-μm channel ($\rho^{*}{}_{2.13}$) are considered as dark pixels and used for AOD retrieval. However, the DT algorithm had been improved many times through the parameters of ($\mathrm{NDVI}_{\mathrm{SWIR}}$) and scattering angle to obtain high retrieval precision [21], [32]. Moreover, the DT algorithm has been the main AOD retrieval algorithm for MODIS AOD products (MOD04). MOD04 products define different aerosol types through cluster analysis using the AERONET observations of aerosol optical parameters over all sites in a global map for each season. AOD retrieval was subsequently calculated via a look-up table (LUT). The expected error (EE) of MOD04 C5 and C6 DT AOD retrievals is $\pm$ (0.05 + 15%) over land at 10-km resolution [32]–[35].

B. MODIS DB Aerosol Retrieval Algorithm Over Land

The DT algorithm over land is not designed for aerosol retrieval over bright surfaces. To address this problem, the DB algorithm was proposed by Hsu *et al.* [22], [23] based on the finding that the surface reflectance in the blue channels (i.e., 0.412 and 0.47 μm) remains low and largely stable over bright surfaces, even in desert areas. The surface reflectance for aerosol retrieval is estimated for the 0.412-, 0.47-, and 0.65-μm channels based on a precalculated seasonal surface reflectance database created from the SeaWiFS surface reflectance products using the

minimum synthesis technique [24]. Since its development, the DB algorithm has been improved in three main aspects. These include the surface reflectance estimation, which takes advantage of the combination of the surface reflectance database and the NDVI and uses a hybrid approach to determine the surface reflectance over different land covers; aerosol model selection, which uses a similar method as the DT algorithm with updated AERONET site data; and cloud screening schemes. The DB algorithm allows AOD retrieval for all dark and bright surfaces except those of oceans and snow/ice areas [22]–[24]. The DB algorithm was chosen to produce the MOD04 C5.1 and C6 AOD products with a 10-km spatial resolution, and the EE is $\pm$ (0.05 + 20%) over land [24]. Moreover, by combining the application of DB and DT algorithms in different regions, the MOD04 C6 aerosol products provided a new DT&DB AOD dataset, which was produced using three separate retrieval algorithms: DT over vegetated/dark-soiled land, DT over ocean, and DB over desert/arid land. To produce this dataset, a map of climatology data from the MODIS-derived, monthly, gridded NDVI product (MYD13C2) is used to determine which algorithm takes precedence [24], [36].

C. MODIS HARLS Over Land

In this study, a new HARLS algorithm to retrieve AOD from MODIS data over land is proposed based on a precalculated monthly land surface reflectance database (LSRD). The HARLS AOD retrievals involve two assumptions: 1) the surface is Lambertian, and 2) the surface reflectance remains unchanged during a certain period for most features [20], [24]. The main difference among the MOD04 DT, DB, and HARLS algorithms is the method employed to estimate the land surface reflectance. The DT algorithm uses the fixed relationships between the blue/red and midinfrared channels to estimate the MODIS land surface reflectance, whereas DB uses a seasonal LSRD created from the SeaWiFS surface reflectance products [22]–[24]. However, HARLS uses a monthly LSRD constructed using long time series of the MODIS surface reflectance products (MOD09A1) to estimate the land surface reflectance. This approach can eliminate the affection produced from the different spectral responses of two different satellite sensors. In addition, there are some other differences among the algorithms regarding the assumption of aerosol types and construction of the LUT.

1) Surface Reflectance Estimation Over Land: Land surface reflectance (LSR) is one of the most important factors affecting the accuracy of AOD retrieval from remote sensing measurements. Previous studies showed that the simulated relationship between AOD and TOA reflectance in the blue band (0.47 μm) of MODIS data demonstrates that the TOA reflectance shows an obvious increase in the AOD, even when the surface reflectance is much higher (up to 0.15) than the value of the dark surfaces in the DT algorithm, which is usually less than 0.04 [20]. Therefore, AOD retrieval can be achieved if the LSR can be estimated accurately.

In this study, a new land surface reflectance estimation method for AOD retrieval is proposed based on the MOD09A1 surface reflectance products. A prior LSRD is constructed using the minimum synthesis technique to provide the actual surface reflectance in the MODIS blue band (0.47 μm) for AOD retrieval. MOD09A1 is the eight-day gridded Level 3 product of the MOD09 series of surface reflectance and includes seven bands covering the visible to near-infrared wavelengths at a spatial resolution of 500 m. The MOD09A1 product provides the best possible L2G observation during an eight-day period, which is selected based on high observation coverage, low view angle, the absence of clouds, cloud shadows, and the absence of aerosol loading. This selection procedure effectively reduces the effect of surface and cloud contamination. The atmospheric correction accuracy is typically $\pm$ $(0.005 + 0.05^{*}\rho)$ under favorable conditions [37].

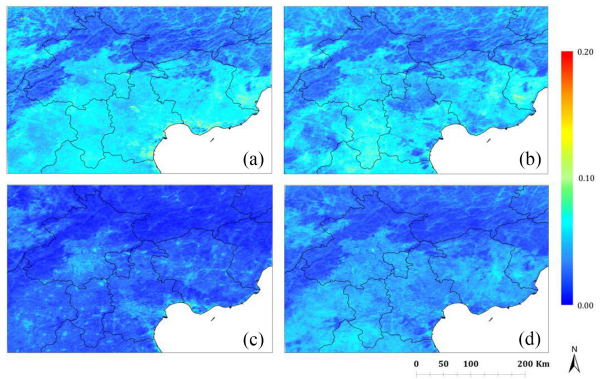

Fig. 1. Monthly land surface reflectance images in the blue band (0.47 μm) in (a) January 2014, (b) April 2014, (c) July 2014, and (d) October 2014.

MOD09A1 surface reflectance products from 2013 to 2014 were collected to construct the LSRD, and a one-month LSRD was created for the AOD retrieval. For each year, the lowest surface reflectance for each pixel in the four images from a given month was chosen as the pixels for the one-month series:

$$I(i,j) = \text{Min}\left(I_1(i,j), I_2(i,j), I_3(i,j), I_4(i,j)\right) \quad (4)$$

where I represents the synthetic image, I_1, I_2, I_3, and I_4 represent four MOD09A1 images in a given month, and i and j represent the row and column, respectively, in an image.

Fig. 1 shows four land surface reflectance images over the Jing-Jin-Ji region from the synthetic LSRD in January 2014, April 2014, July 2014, and October 2014. From Fig. 1, we can see that the surface reflectance is much higher in January than in July and higher in bright urban areas than in the surrounding areas. The surface reflectance varies extensively in the study area due to the presence of complex structures. The blue-band surface reflectance distribution is analyzed according to the statistics of the surface reflectance images over the Jing-Jin-Ji region. In most areas, the blue-band LSR is low, and nearly 98% of the surface reflectance is generally less than 0.10 in the blue band (0.47 μm) except for the surface reflectance in a few extremely bright areas, such as bare land and unused land. Therefore, the surface reflectance in the blue band can be estimated for AOD retrieval from MODIS using the constructed LSRD.

2) Aerosol Type Assumption Over Land: The composition of the aerosol model is constantly changing in different areas, and the selection of an aerosol model is an important issue in

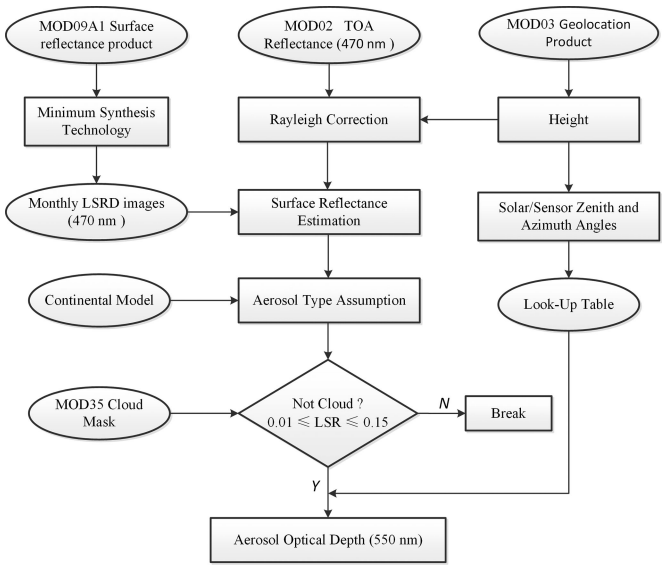

Fig. 2. Flowchart of the HARLS over land.

AOD retrieval. For MOD04 aerosol products, different aerosol models are defined through the AERONET sites in a global map for each season and include continental, absorbing, moderate absorbing, and weak absorbing aerosol models with different optical properties, such as the single scattering albedo and asymmetry parameter [38]. However, previous studies have shown that continental aerosols can be used to broadly describe the aerosol conditions for the research area [19], [20], [39], [40]. Therefore, we assume the dominant aerosol type is continental and its detailed optical properties defined at 550 nm can be found in [20].

3) LUT Construction: Similar to MODIS aerosol retrieval algorithms, HARLS also needs a LUT to perform AOD retrieval. The LUT is built using the 6S model (second simulation of the satellite signal in the solar spectrum) and carefully considering the aerosol scattering and gaseous (including H_2O, O_3, O_2, and CO_2) absorption among other factors [41]. This model has been widely used for the LUT calculation for AOD retrieval from many sensors. However, for HARLS, there are some differences from the MODIS DT and DB algorithms in LUT construction that involve parameter settings, such as a wider range and finer intervals of aerosols or solar/sensor zenith angles [38]. The detailed parameter settings for the continental model in the LUT can be found in [20].

4) AOD Retrieval: The nonmasked pixels are evaluated for brightness; pixels in the LSRD with LSR values between 0.01 and 0.15 are selected for aerosol retrieval ($0.01 \leq \mathrm{LSR} \leq 0.15$). The daily MOD35 cloud mask product is selected to filter unsuitable cloud pixels. The pixels are evaluated individually to identify those pixels suitable for aerosol retrieval. Finally, the TOA reflectance from the MOD021KM data from 2013 to 2014 with the corresponding LSR image from the LSRD, MOD35 cloud mask product, MOD03 geolocation product, and LUT are used to conduct the AOD retrieval for the MODIS data. Fig. 2 shows a flowchart of HARLS over land.

III. Evaluation Methods

A. AERONET Ground-Measured Data

The AERONET is a worldwide network of calibrated ground-based aerosol sites collected with Sun photometers established by NASA, the French Centre National de la Recherché Scientifique, and numerous other partners. This system provides long-term continuous and accessible public aerosol records every 15 min, which have a lower uncertainty value of $\sim$0.01 [42], [43]. Here, the AERONET AOD ground measurements of Level 1.5 (cloud screened) for Beijing_CAMS, Beijing_RADI, and XiangHe sites and Level 2.0 (cloud screened and quality assured) for Beijing site from the years 2013 and 2014 were collected and used for evaluation purposes. Three sites, Beijing, Beijing_CAMS, and Beijing_RADI, are located in bright urban areas, whereas the XiangHe site has a relatively lower reflectance and is less bright than the other urban sites in Beijing due to agricultural lands adjacent to the XiangHe site. As the MODIS AOD retrievals are at the wavelength of 550 nm, the AODs at 440, 500, and 675 nm from AERONET were interpolated using the Ångström Exponent method to obtain the AOD ground observations at 550 nm to match with the AOD retrievals [44], [45].

B. Evaluation Methods

The HARLS AOD was retrieved at a spatial resolution of 1000 m using MOD021KM and was compared and validated with AERONET AOD ground-based observations and MOD04 aerosol products (C5 and C6 at 10-km spatial resolution). For comparison purposes, AOD observations with only the highest quality flag (QF = 3) from C5 DT, C6 DT, C6 DB and the combined C6 DT&DB AOD at 10-km resolution were obtained.

To reduce the effects of accidental errors and individual values, the average of at least two AERONET AOD measurements at the four sites within $\pm$ 30 min of the MODIS overpass times were matched with different aerosol product retrieved AODs within a sampling window of 3×3 pixels (average of 9 pixels) centered on the AERONET sites [10]–[13], [21]–[24], [33]. This procedure included the average of 3×3 km^2 spatial areas for the HARLS AODs at a resolution of 1 km and the average of 30×30 km^2 spatial areas for the MOD04 AODs at a resolution of 10 km.

Moreover, in this study, deming regression, which is an orthogonal regression technique, was used to estimate the slope and intercept of the datasets, and the Pearson product-moment correlation coefficient (R, (5)) was selected to analyze the correlation between retrievals and measured values. Additionally, the expected error (EE, (6)) over land, relative mean bias (RMB, (7)), mean absolute error (MAE, (8)), mean relative error (MRE, (9)), and root-mea- square error (RMSE, (10)) were selected to evaluate the uncertainty in the aerosol retrievals

$$\mathrm{R} = \frac{\sum_{i=1}^{n} (x_i - \bar{x})(y_i - \bar{y})}{\sqrt{\sum_{i=1}^{n} (x_i - \bar{x}) \sum_{i=1}^{n} (y_i - \bar{y})}} \tag{5}$$

$$\mathrm{EE} = \pm (0.05 + 0.2\mathrm{AOD}_{\mathrm{AERONET}}) \tag{6}$$

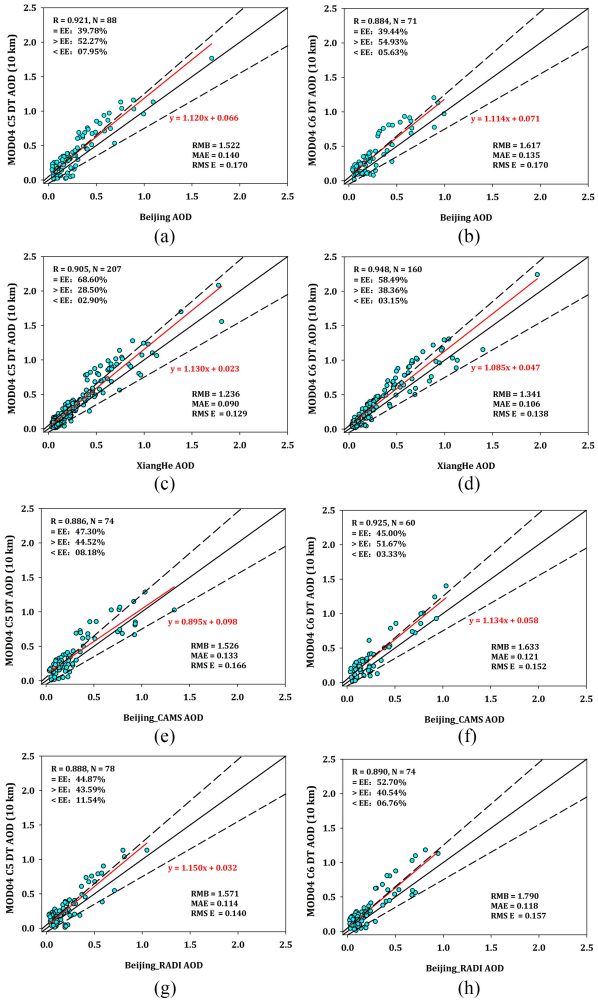

Fig. 3. Comparisons of MOD04 C5/C6 DT (10 km) AOD products with AERONET AODs at (a) Beijing (C5), (b) Beijing (C6), (c) XiangHe (C5), (d) XiangHe (C6), (e) Beijing_CAMS (C5), (f) Beijing_CAMS (C6), (g) Beijing_RADI (C5), and (h) Beijing_RADI (C6) sites. The dashed lines represent EE lines, the black solid line is the 1:1 line, and the red solid line is the regression line.

$$\mathrm{RMB} = \frac{1}{n}\sum_{i=1}^{n}\left|\mathrm{AOD}_{\mathrm{Retrieval}}/\mathrm{AOD}_{\mathrm{AERONET}}\right| \tag{7}$$

$$\mathrm{MAE} = \frac{1}{n}\sum_{i=1}^{n}\left|\mathrm{AOD}_{\mathrm{Retrieval}} - \mathrm{AOD}_{\mathrm{AERONET}}\right| \tag{8}$$

$$\mathrm{MRE} = \frac{1}{n}\sum_{i=1}^{n}\frac{\left|\mathrm{AOD}_{\mathrm{Retrieval}} - \mathrm{AOD}_{\mathrm{AERONET}}\right|}{\mathrm{AOD}_{\mathrm{AERONET}}} \tag{9}$$

$$\mathrm{RMSE} = \sqrt{\frac{1}{n}\sum\nolimits_{i=1}^{n}\left(\mathrm{AOD}_{\mathrm{Retrieval}} - \mathrm{AOD}_{\mathrm{AERONET}}\right)^2}. \tag{10}$$

IV. Results and Analysis

The MOD04 C5 DT, C6 DT, DB and the combined C6 DT&DB AOD at 10 km and the HARLS AOD at 1000 m from 2013 to 2014 are collected and plotted against the AERONET AOD ground observations at the four sites, Beijing, XiangHe, Beijing_CAMS, and Beijing_RADI, located in the Jing-Jin-Ji region (see Figs. 3–8). The validation of the different MODIS aerosol retrieval algorithms is discussed in detail in the following sections, and the evaluation statistics are provided in Table I.

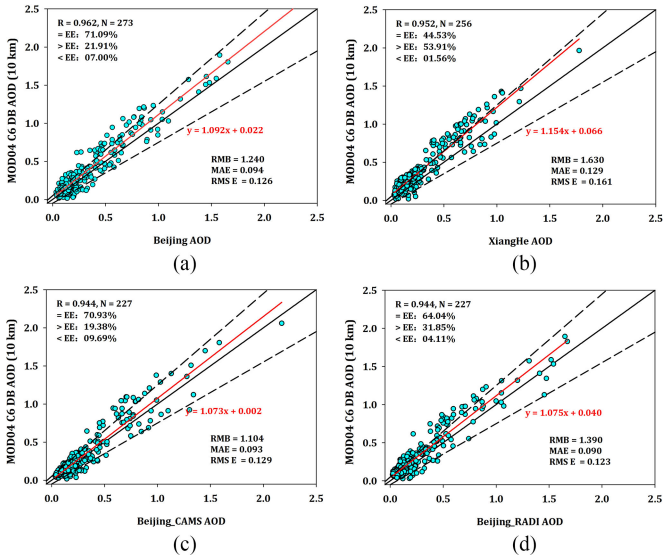

Fig. 4. Comparison of the MOD04 C6 DB AOD product (10 km) with AERONET AODs at (a) Beijing, (b) XiangHe, (c) Beijing_CAMS, and (d) Beijing_RADI sites.

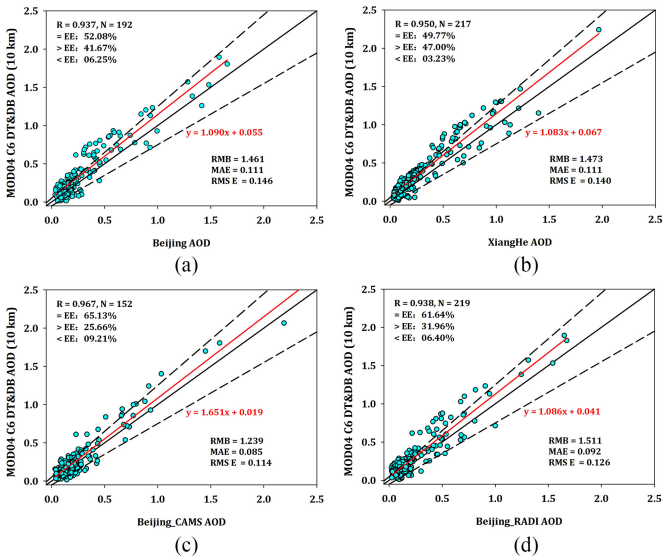

Fig. 5. Comparison of the MOD04 C6 DT&DB AOD product (10 km) with AERONET AODs at (a) Beijing, (b) XiangHe, (c) Beijing_CAMS, and (d) Beijing_RADI sites.

A. Evaluation of MOD04 C5 and C6 DT Retrievals (10 km)

Fig. 3 shows a comparison between the MOD04 C5 DT and C6 DT AOD retrievals (10 km) and the Beijing, XiangHe, Beijing_CAMS, and Beijing_RADI AERONET AOD results.

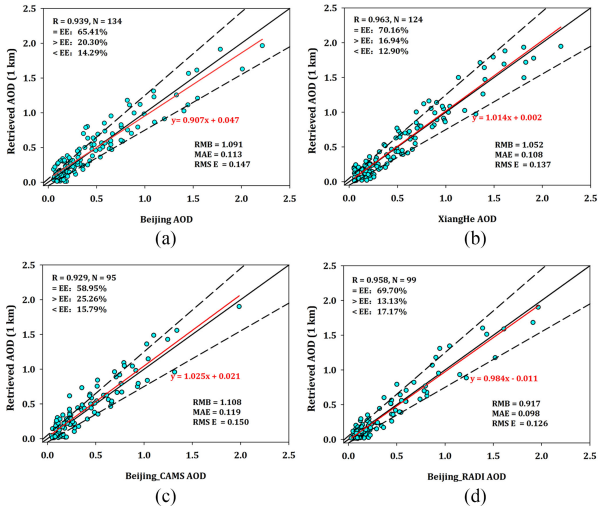

Fig. 6. Comparison of the HARLS AOD product (1 km) with AERONET AODs at (a) Beijing, (b) XiangHe, (c) Beijing_CAMS, and (d) Beijing_RADI sites.

The MODIS DT algorithm can only be used to retrieve AOD in densely vegetated areas, resulting in few validation collocations, with a valid range and contribution mostly between 0.0 and 1.0 (60–90 points for Beijing, Beijing_CAMS and Beijing_RADI). However, due to nearby agricultural lands, the XiangHe site is less bright than the other urban sites in Beijing, leading to larger collocation numbers (207 points for C5 DT and 160 points for C6 DT). Although the C5 DT AOD retrievals have high correlation with the AERONET AOD measurements, only 40%–50% of the collocations fall within the EE, and 40%–55% of the collocations fall above the EE, leading to an overestimation of 20%–60% (RMB $\approx 1.20 - 1.60$) and a large uncertainty. The C6 DT AOD retrievals show a better correlation ($R \approx 0.88 - 0.95$) than the C5 DT AOD retrievals ($R \approx 0.88 - 0.92$) with the AERONET AOD, and 40%–55% of the collocations fall within the EE with a low MRE. Compared with C5 DT, C6 DT has an average of 1%–5% less overestimation and is closer to the 1:1 line.

When AOD > 0.4, the C6 DT AOD has a higher correlation with AERONET AOD than does the C5 DT AOD. However, the DT algorithm exhibits overestimation during clear and polluted days, when AOD > 0.4, and 80% of the collections are overestimated. When AOD < 0.4, more than 50% of the aerosol retrievals are overestimated significantly. This overestimation arises primarily as a result of the accuracy of the surface reflectance determination and the aerosol model applied. The verification results show that MOD04 C5 DT and C6 DT aerosol products are not suitable for remote-sensing application research on atmospheric aerosols in typical local areas; thus, there is important theoretical and practical significance for proposing a high-precision method of aerosol retrieval.

B. *Evaluation of MOD04 C6 DB Retrievals (10 km)*

Fig. 4 shows a comparison between the MOD04 C6 DB AODs (10 km) and the AERONET AODs at the four sites. Because the C6 DB algorithm can retrieve AOD over both dark and

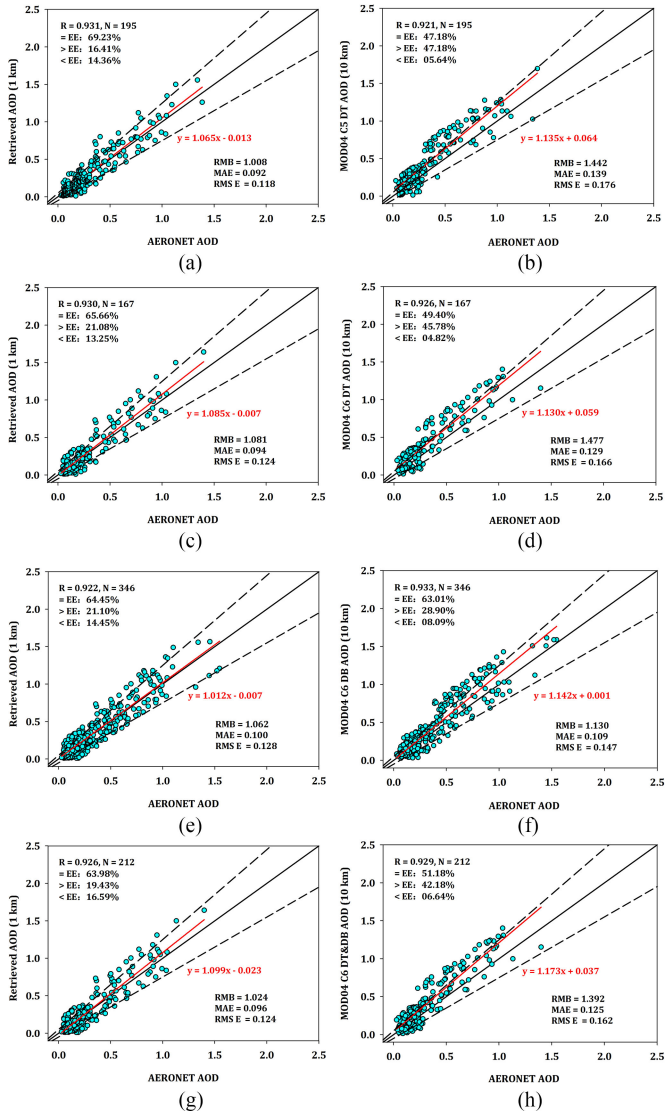

Fig. 7. Comparisons between the HARLS AOD product (1 km) (a), (c), (e), (g) and MOD04 C5 DT (b), C6 DT (d), C6 DB (f), C6 DT&DB (h) AOD products (10 km) as validated relative to AERONET AODs in the Jing-Jin-Ji region for the years 2013–2014.

bright surfaces, the DB algorithm makes a greater contribution (ranging from 0.0 to 2.0) than the DT algorithm (AOD $\approx 0.0 - 1.0$) and can achieve aerosol retrieval during high-pollution days (AOD > 1.0). Thus, the C6 DB collections (Beijing $= 273$, Beijing_CAMS $= 227$, Beijing_RADI $= 227$) are significantly more numerous than those of the DT algorithm and almost four times more numerous than those of C6 DT algorithm (Beijing $= 71$, Beijing_CAMS $= 60$, Beijing_RADI $= 74$) in urban areas. The verification results show that the C6 DB AOD has a higher correction ($R \approx 0.94 - 0.97$) with the AERONET AOD results compared with the DT algorithm ($R \approx 0.88 - 0.95$), and approximately 50%–70% of the collections meet the error requirement of falling within the EE. The C6 DB retrievals have lower RMSE, MRE, and MAE values and 20%–30% less average overestimation than do the C5 DT retrievals, causing them to plot closer to the 1:1 line (RMB $\approx 1.1 - 1.4$). However, although the DB algorithm

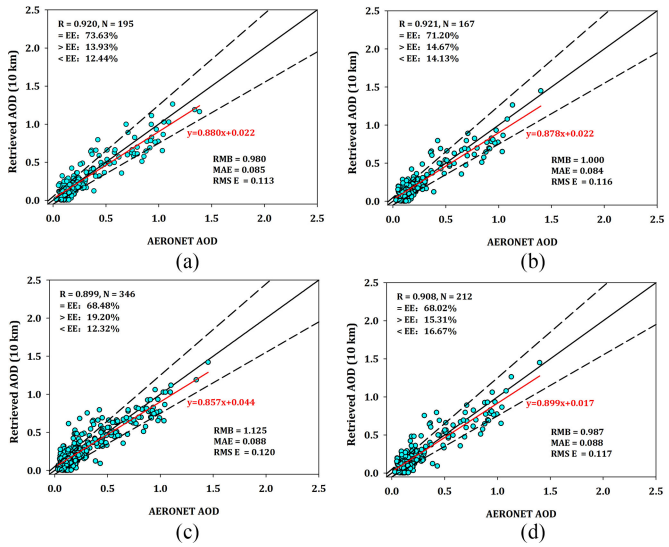

Fig. 8. Comparisons between the HARLS AOD product (10 km) and MOD04 C5 DT (a), C6 DT (b), C6 DB (c), C6 DT&DB (d) AOD products (1 km) as validated relative to AERONET AODs in the Jing-Jin-Ji region for the years 2013–2014.

shows a higher correlation with the AERONET AOD data than does the DT algorithm, it has higher RMSE and MRE values than the DT algorithm (RMB $\approx 1.2 - 1.3$), with less than 15%–20% of collections falling above and below the EE and causing an overestimation of 30%–40% (RMB $= 1.63$) relative to the AERONET AODs at the XiangHe site.

C. Evaluation of MOD04 C6 DT&DB Retrievals (10 km)

Fig. 5 shows a comparison between the MOD04 C6 DT&DB AOD retrievals (10 km) and the AERONET AOD data from the four sites. In Fig. 5, the DT&DB algorithm exhibits the same wide contribution range (AOD $\approx 0.0 - 2.0$) as the DB algorithm, and the DT&DB AOD results show high consistency with the AERONET AODs ($R \approx 0.93 - 0.97$), with approximately 50%–70% of the collections falling within the EE. Moreover, DT&DB has good consistency with DB in urban areas but yields lower MRE, MAE, and RMSE values than DB at the XiangHe site. Compared with the DT algorithm, the DT&DB algorithm shows a higher correlation with the AERONET AOD data, with lower MRE, MAE, and RMSE values, and approximately 10%–20% more of the collections falling within the EE. The DT&DB algorithm has an overall higher AOD retrieval precision and compensates for the insufficiency of the DB algorithm in dense vegetation areas. Thus, it can be used for quantitative aerosol studies and applications in complex areas.

D. Evaluation of HARLS Retrievals (1000 m)

Fig. 6 shows the comparison results between the AOD retrievals at 1-km spatial resolution using the HARLS and the AERONET measurements from the four sites. The dotted lines represent the EE lines, the black dashed lines are the 1:1 lines, and the red solid lines represent the regression lines. The retrieved AODs range from 0.0 to 2.0, and the wide range distribution can meet the validation requirements during periods of low and high aerosol concentrations. Fig. 6 shows that more than 94% of the observations have AOD values less than 1.5, and 4%, 6%, 1%, and 4% of the observations had AOD values greater than 1.5 at the Beijing, XiangHe, Beijing_CAMS, and Beijing_RADI sites, respectively. The validation results show that the HARLS-retrieved AODs are highly consistent with those from the AERONET stations ($R \approx 0.93 - 0.96$) and are evenly distributed on both sides of the black solid line (1:1 line). The validation results have a slope close to 1 (slope $\approx 0.90 - 1.02$), a small offset (intercept $\approx 0.00 - 0.04$), and a small RMB ($\approx 0.90 - 1.10$) and MAE ($\approx 0.09 - 0.12$). The HARLS algorithm can realize aerosol retrieval under both low-pollution (AOD < 0.5) and high-pollution conditions (AOD > 1.0), with more than 65% of the retrievals falling within the EE (Beijing $= 65.41\%$, XiangHe $= 70.16\%$, and Beijing_RADI $= 69.70\%$). This new algorithm can achieve aerosol retrieval in both bright and dark surfaces with high accuracy.

E. Comparison Between HARLS and MOD04 AOD Products

The HARLS AOD product and different MOD04 AOD products, including C5 DT (10 km), C6 DT (10 km), C6 DB (10 km), and C6 DT&DB (10 km), as well as AERONET AOD observations from the same time and area are obtained for the four AERONET sites in the Jing-Jin-Ji region. Fig. 7 shows the results of comparisons between the HARLS AODs (1 km) and MOD04 AODs (10 km) as validated relative to the AERONET AODS, and Fig. 8 shows the results of comparisons between the HARLS AODs (10 km) and MOD04 AODs (10 km) as validated relative to the AERONET AODs. Table II shows the validation statistics of the HARLS AODs (1 and 10 km) and MOD04 AODs (10 km) based on different algorithms.

In Fig. 7 and Table II, 195 collections for HARLS & C5 DT, 167 collections for HARLS & C6 DT, 346 collections for HARLS & C6 DB, and 212 collections for HARLS & C6 DT&DB are comparatively validated relative to the AERONET AODs from the four sites in the Jing-Jin-Ji region. Comparison results show that the HARLS retrievals can achieve a high consistency with the AERONET measured AODs ($R \approx 0.92 - 0.94$), with the best slope close to 1 (slope $\approx 1.00 - 1.10$), a small positive offset (intercept $\approx 0.00 - 0.02$), and a low RMSE ($\approx 1.11 - 1.13$), MAE ($\approx 0.09 - 0.10$), and MRE ($\approx 37.89 - 46.38$). Approximately 60%–70% of the collocations fall within the EE, and less than 22% of the collocations fall above the EE, causing an overestimation of 0%–10% (RMB $\approx 1.00 - 1.10$) relative to the AERONET AOD results. Therefore, HARLS can accurately retrieve AOD in both low and high surface reflectance areas, even on heavily polluted days (AOD > 1.0). The comparisons show that the HARLS AOD products showed an overall higher accuracy than that of the MOD04 AOD products; these products are less biased than the DT and DT&DB AOD products and marginally better than MOD04 DB AOD products in the Jing-Jin-Ji region.

To better understand why the HARLS AODs have less bias than the MOD04 AODs, the HARLS AODs at 1-km resolution are aggregated into 10 km using the same resampling approach

TABLE I
EVALUATION STATISTICS OF MOD04 C5 DT, C6 DT, C6 DB, C6 DT AND DB (10 KM), AND HARLS AOD (1 KM) RETRIEVALS WITH RESPECT TO AERONET AODS AT BEIJING, XIANGHE, BEIJING_CAMS, AND BEIJING_RADI STATIONS

AERONET	Algorithm	N	RMB	MAE	MRE	RMSE	=EE %	>EE %	<EE %
Beijing	C5 DT	88	1.522	0.140	75.069	0.170	39.78	52.27	07.95
	C6 DT	71	1.617	0.135	76.866	0.170	39.44	54.93	05.63
	C6 DB	273	1.240	0.094	43.103	0.126	71.09	21.91	07.00
	C6 DT&DB	192	1.461	0.111	61.682	0.146	52.08	41.67	06.25
	HARLS	134	1.091	0.113	40.567	0.147	65.41	20.30	14.29
XiangHe	C5 DT	207	1.236	0.090	42.680	0.129	68.60	28.50	02.90
	C6 DT	160	1.341	0.106	47.785	0.138	58.49	38.36	03.15
	C6 DB	256	1.630	0.129	69.527	0.161	44.53	53.91	01.56
	C6 DT&DB	217	1.473	0.111	58.748	0.140	49.77	47.00	03.23
	HARLS	124	1.052	0.108	37.294	0.137	70.16	16.94	12.90
Beijing_CAMS	C5 DT	74	1.526	0.133	71.092	0.166	47.30	44.52	08.18
	C6 DT	60	1.633	0.121	80.135	0.152	45.00	51.67	03.33
	C6 DB	227	1.104	0.093	34.926	0.129	70.93	19.38	09.69
	C6 DT&DB	152	1.239	0.085	47.424	0.114	65.13	25.66	09.21
	HARLS	95	1.108	0.119	44.424	0.150	58.95	25.26	15.79
Beijing_RADI	C5 DT	78	1.571	0.114	82.960	0.140	44.87	43.59	11.54
	C6 DT	74	1.790	0.118	96.103	0.157	52.70	40.54	06.76
	C6 DB	292	1.390	0.090	51.173	0.123	64.04	31.85	04.11
	C6 DT&DB	219	1.511	0.092	65.937	0.126	61.64	31.96	06.40
	HARLS	99	0.917	0.098	40.250	0.126	69.70	13.13	17.17

TABLE II
EVALUATION STATISTICS OF MOD04 C5 DT, C6 DT, C6 DB, C6 DT AND DB (10 KM), AND HARLS (1 KM AND 10 KM) AOD RETRIEVALS WITH RESPECT TO AERONET AODS FROM THE SAME TIME AND STATIONS IN THE JING-JIN-JI REGION

Algorithm	N	R	RMB	MAE	MRE	RMSE	=EE %	>EE %	<EE %
C5 DT	195	0.921	1.442	0.139	58.682	0.176	47.18	47.18	05.64
HARLS (1 km)	195	0.931	1.008	0.092	40.657	0.118	69.23	16.41	14.36
HARLS (10 km)	195	0.920	0.980	0.085	47.614	0.113	73.63	13.93	12.44
C6 DT	167	0.926	1.477	0.129	61.134	0.166	49.40	45.78	04.82
HARLS (1 km)	167	0.930	1.081	0.094	46.124	0.124	65.66	21.08	13.26
HARLS (10 km)	167	0.921	1.000	0.084	52.627	0.116	71.20	14.67	14.13
C6 DB	346	0.933	1.130	0.109	37.886	0.147	63.01	28.90	08.09
HARLS (1 km)	346	0.922	1.062	0.100	51.617	0.128	64.45	21.10	14.45
HARLS (10 km)	346	0.899	1.125	0.088	56.447	0.120	68.48	19.20	12.32
C6 DT&DB	212	0.929	1.392	0.125	55.962	0.162	51.18	42.18	06.64
HARLS (1 km)	212	0.926	1.024	0.096	49.156	0.124	63.98	19.43	16.59
HARLS (10 km)	212	0.908	0.987	0.088	53.752	0.117	68.02	15.31	16.67

[32], [33] used with the MOD04 AOD products and compared with the MOD04 AODs with respect to the AERONET AODs. Fig. 8 shows the validations of HARLS & C5 DT, HARLS & C6 DT, HARLS & C6 DB, and HARLS & C6 DT&DB with respect to the AERONET-measured AODs from the four sites. The HARLS AOD retrievals at 10-km resolution have an overall high consistency ($R \approx 0.90 - 0.92$), and approximately 68%–74% of the collocations fall within the EE, causing an underestimation or overestimation of 3%–13% (RMB $\approx 0.98 - 1.13$) relative to the AERONET AODs. In addition, the HARLS AODs showed good slopes ranging from 0.85 to 0.90, with small offsets (intercept $\approx 0.00 - 0.03$) and low RMSE ($\approx 0.11 - 0.12$) and MAE ($\approx 0.08 - 0.09$) values (see Table II). In general, the HARLS AODs at 10-km spatial resolution show an overall lower accuracy and higher uncertainty than the HARLS AODs at 1-km resolution; however, they remain much better and less biased than the MOD04 DT and DT&DB AOD products and marginally better than the DB AOD products. Due to the improvement of the signal-to-noise ratio of the images [32], [33], resampling to a low spatial resolution can improve the accuracy of HARLS AOD products to some extent, but the overall effect is small. However, the accuracy differences among the different MODIS AOD products are mainly due to differences in not only the surface reflectance estimation but also the assumptions of the aerosol models [45]–[48].

F. Spatial Distribution Comparison of MODIS Aerosol Products Over the Jing-Jin-Ji Region

In this paper, two images with different aerosol loads—July 14, 2014 and July 26, 2014—are selected to represent the aerosol distribution and are used for comparisons among the MOD04 C6 DT (10 km), C6 DB (10 km), C6 DT&DB (10 km), and HARLS (1000 m) AOD products (Fig. 9). Fig. 9(a) and (b) shows the standard MODIS false-color images (RGB: 213) during periods of low and high aerosol loads over the Jing-Jin-Ji region and its surroundings. Fig. 9(c) and (d) shows the spatial distribution of the C6 DT AODs. The DT algorithm is unable to retrieve AODs

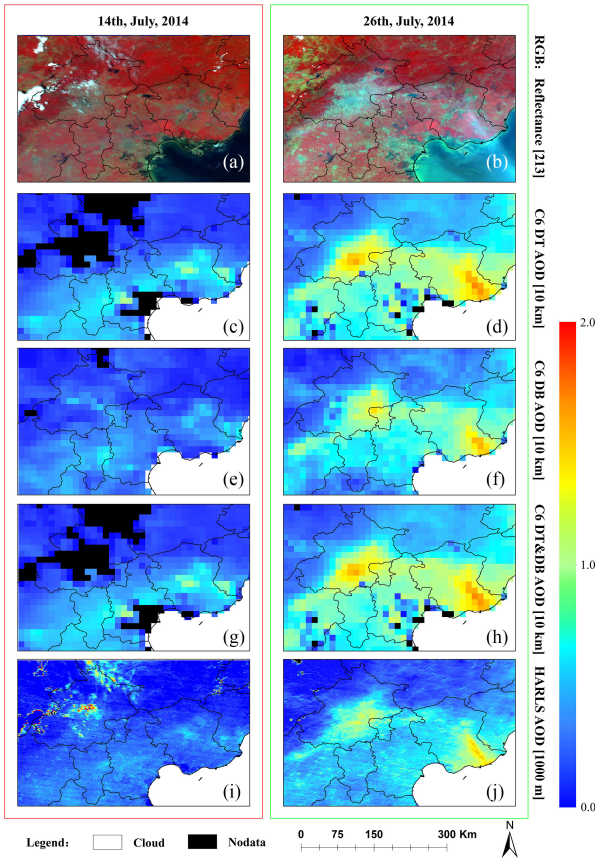

Fig. 9. Distributions of the HARLS and MOD04 aerosol products in the Jing-Jin-Ji region under low and high aerosol loads on July 14, 2014 and July 26, 2014.

in bright urban areas and shows a large number of missing values, with poor spatial continuity overall. However, the DB algorithm can achieve aerosol retrieval in urban areas, even with high pollution, and performs better over bright areas, resulting in a better spatial continuity than the DT algorithm (see Fig. 9(e) and (f)). The DT&DB algorithm performs similar to the DT algorithm but nonetheless has a large number of missing values in bright areas, with relatively poor spatial continuity (see Fig. 9(g) and (h)). The HARLS retrievals achieve a more continuous AOD distribution, even in bright areas such as the centers of urban areas with buildings and roads, which have a high degree of reflectance and complex patterns. The comparison results showed that HARLS can realize AOD retrievals over both dark and bright areas, and it can describe the aerosol distribution and variability in greater detail at a higher spatial resolution (1000 m) than can the current MOD04 AOD products at 10-km spatial resolution under both low and high aerosol loads (see Fig. 9(i) and (j)).

V. Conclusion

Many aerosol retrieval algorithms based on the remote sensing technology have been developed for different satellite sensors. The purpose of this paper is to evaluate different MODIS AOD products, including MOD04 C5 DT, C6 DT, DB, and DT&DB AOD products at 10-km spatial resolution, and the new AOD product produced by the new HARLS at 1-km spatial resolution from 2013 to 2014 over the Beijing-Tianjin-Hebei (Jing-Jin-Ji) region in China. This region features complex land surface structures and serious air pollution. The corresponding AERONET AOD observations for the Beijing, XiangHe, Beijing_CAMS, and Beijing_RADI sites were obtained for validation purposes. Evaluation and comparison of the results showed that the C6 DT algorithm showed an AOD retrieval quality similar to that of the C5 DT algorithm. However, the DT algorithm overestimated more than 47% of the aerosol retrievals during both clear and polluted days and was unable to retrieve AODs over bright areas. The DB AODs showed a higher correlation with the AERONET AODs ($R \approx 0.93$) than did the DT AODs, with lower MAE and RMSE values, and the DB algorithm was able to retrieve AODs over both dark and bright surfaces. The DT&DB AODs exhibited a high consistency with the AERONET AODs and yielded better results overall compared with the DT AODs. The HARLS AODs showed a higher correlation with AERONET AODs, with lower RMSE ($\approx 0.11 - 0.1$) and MAE values ($\approx 0.09 - 0.10$) and an overestimation of only 0%–10% (RMB $\approx 1.00 - 1.10$) than MOD04 AOD products. HARLS yielded more accurate aerosol retrievals than either DB or DT algorithms over the Jing-Jin-Ji region, and it can produce a complete and detailed aerosol spatial distribution for both low and high aerosol loads. The main reason cannot all be attributable to the differences of surface reflectance estimation and aerosol model assumption, but also to the higher spatial resolution used in the retrievals. The HARLS AOD products will be useful in quantitative aerosol studies and urban air quality monitoring in the future.

References

[1] C. N. Cruz and S. N. Pandis, "A study of the ability of pure secondary organic aerosol to act as cloud condensation nuclei," *Atmos. Environ.*, vol. 31, no. 15, pp. 2205–2214, 1997.

[2] V. Ramanathan *et al.*, "Indian Ocean experiment: An integrated analysis of the climate forcing and effects of the great Indo-Asian haze," *J. Geophys. Res.*, vol. 106, no. D22, pp. 28371–28398, 2001.

[3] Y. J. Kaufman, D. Tanré, and O. Boucher, "A satellite view of aerosols in the climate system," *Nature*, vol. 419, no. 6903, pp. 215–223, 2002.

[4] J. Sun and P. Ariya, "Atmospheric organic and bio-aerosols as cloud condensation nuclei (CCN): A review," *Atmos. Environ.*, vol. 40, no. 5, pp. 795–820, 2006.

[5] R. N. Colvile, E. J. Hutchinson, J. S. Mindell and R. F. Warren, "The transport sector as a source of air pollution," *Atmos. Environ.*, vol. 35, no. 9, pp. 1537–1565, 2001.

[6] C. A. Pope *et al.*, "Lung cancer, cardiopulmonary mortality, and long-term exposure to fine particulate air pollution," *JAMA*, vol. 287, no. 9, pp. 1132–1141, 2002.

[7] M. Kocifaj, H. Horvath, O. Jovanović, and M. Gangl, "Optical properties of urban aerosols in the region Bratislava-Vienna I. Methods and tests," *Atmos. Environ.*, vol. 40, no. 11, pp. 1922–1934, 2006.

[8] J. F. Gent *et al.*, "Symptoms and medication use in children with asthma and traffic-related sources of fine particle pollution," *Environ. Health Perspect.*, vol. 117, no. 7, pp. 1168–1174, 2009.

[9] D. Huang, J. Xu, and S. Zhang "Valuing the health risks of particulate air pollution in the Pearl River Delta, China," *Environ. Sci. Policy*, vol. 15, no. 1, pp. 38–47, 2012.

[10] Y. J. Kaufman *et al.*, "Passive remote sensing of tropospheric aerosol and atmospheric correction for the aerosol effect," *J. Geophys. Res.*, vol. 102, no. D14, pp. 16815–16830, 1997a.

[11] Y. J. Kaufman, D. Tanré, L. A. Remer, E. F. Vermote, A. Chu, and B. N. Holben, "Operational remote sensing of tropospheric aerosol over land from EOS moderate resolution imaging spectroradiometer," *J. Geophys. Res.*, vol. 102, no. D14, pp. 17051–17067, 1997b.

[12] O. Torres, P. K. Bhartia, J. R. Herman, A. Sinyuk, P. Ginoux, and B. Holben, "A long-term record of aerosol optical depth from TOMS observations and comparison to AERONET measurements," *J. Atmos. Sci.*, vol. 59, no. 3, pp. 398–413, 2002.
[13] O. Torres *et al.*, "Aerosols and surface UV products from ozone monitoring instrument observations: An overview," *J. Geophys. Res.*, vol. 112, no. D24, pp. 177–180, 2007.
[14] M. Riffler, C. Popp, A. Hauser, F. Fontana, and S. Wunderle, "Validation of a modified AVHRR aerosol optical depth retrieval algorithm over Central Europe," *Atmos. Meas. Tech. Discuss.*, vol. 3, no. 5, pp. 1255–1270, 2010.
[15] R. A. Kahn *et al.*, "Multiangle imaging spectroradiometer global aerosol product assessment by comparison with the aerosol robotic network," *J. Geophys. Res.*, vol. 115, no. D23, pp. 6696–6705, 2010.
[16] A. M. Sayer, N. C. Hsu, C. Bettenhausen, M. J. Jeong, B. N. Holben, and J. Zhang, "Global and regional evaluation of over-land spectral aerosol optical depth retrievals from SeaWiFS," *Atmos. Meas. Tech.*, vol. 5, no. 7, pp. 1761–1778, 2012.
[17] J. M. Jackson *et al.*, "Suomi-NPP VIIRS aerosol algorithms and data products," *J. Geophys. Res. Atmos.*, vol. 118, no. 22, pp. 12673–12689, 2013.
[18] H. Liu *et al.*, "Preliminary evaluation of S-NPP VIIRS aerosol optical thickness," *J. Geophys. Res. Atmos.*, vol. 119, no. 7, pp. 3942–3962, 2014, doi: 10.1002/2013JD020360.
[19] L. Sun, C. Sun, Q. Liu, and B. Zhong, "Aerosol optical depth retrieval by HJ-1/CCD supported by MODIS surface reflectance data," *Sci. China Earth Sci.*, vol. 53, no. S1, pp. 74–80, 2010.
[20] L. Sun *et al.*, "Aerosol optical depth retrieval over bright areas using landsat 8 OLI images," *Remote Sens.*, vol. 8, no. 23, pp 1–14, 2016.
[21] R. C. Levy, L. A. Remer, S. Mattoo, E. F. Vermote, and Y. J. Kaufman, "Second generation operational algorithm: Retrieval of aerosol properties over land from inversion of Moderate Resolution Imaging Spectroradiometer spectral reflectance," *J. Geophys. Res.*, vol. 112, no. 13, pp. 1–21, 2007a.
[22] N. C. Hsu, S. C. Tsay, M. D. King, and J. R. Herman, "Aerosol properties over bright-reflecting source regions," *IEEE Trans. Geosci. Remote Sens.*, vol. 42, no. 3, pp. 557–569, Mar. 2004.
[23] C. N. Hsu, S. C. Tsay, M. D. King, and J. R. Herman, "Deep blue inversions of Asian aerosol properties during ACE-Asia," *IEEE Trans. Geosci. Remote Sens.*, vol. 44, no. 11, pp. 3180–3195, Nov. 2006.
[24] N. C. Hsu *et al.*, "Enhanced deep blue aerosol retrieval algorithm: The second generation," *J. Geophys. Res. Atmos.*, vol. 118, no. 16, pp. 9296–9315, 2013.
[25] D. Tanré, P. Y. Deschamps, C. Devaux, and M. Herman, "Estimation of Saharan aerosol optical thickness from blurring effects in thematic mapper data," *J. Geophys. Res.*, vol. 93, no. D12, pp. 15955–15964, 1988.
[26] E. F. Vermote, D. Tanre, J. L. Deuze, M. Herman, and J. J. Morcette, "Second simulation of the satellite signal in the solar spectrum, 6S: An overview," *IEEE Trans. Geosci. Remote Sens.*, vol. 35, no. 3, pp. 675–686, 1997.
[27] M. I. Mishchenko, I. V. Geogdzhayev, B. Cairns, W. B. Rossow, and A. A. Lacis, "Aerosol retrievals over the ocean by use of channels 1 and 2 AVHRR data: Sensitivity analysis and preliminary results," *Appl. Opt.*, vol. 38, no. 36, pp. 7325–7341, 1999.
[28] O. Lado-Bordowsky and I. Le Naour, "Optical paths involved in determining the scattering angle for the scattering algorithm developed in LOWTRAN7," *Int. J. Infrared Millimeter Waves*, vol. 18, no. 9, pp. 1689–1696, 1997.
[29] S. Liang, *Quantitative Remote Sensing of Land Surfaces*. Hoboken, NJ, USA: Wiley, 2005.
[30] B. A. Bodhaine, N. B. Wood, E. G. Dutton, and J. R. Slusser, "On Rayleigh optical depth calculations," *J. Atmos. Ocean. Technol.*, vol. 16, no. 11, pp. 1854–1861, 1999.
[31] A. Bucholtz, "Rayleigh-scattering calculations for the terrestrial atmosphere," *Appl. Opt.*, vol. 34, no. 15, pp. 2765–2773, 1995.
[32] L. A. Remer, S. Mattoo, R. C. Levy, and L. A. Munchak, "MODIS 3 km aerosol product: Algorithm and global perspective," *Atmos. Meas. Tech.*, vol. 6, no. 7, pp. 1829–1844, 2013.
[33] R. C. Levy *et al.*, "The Collection 6 MODIS aerosol products over land and ocean," *Atmos. Meas. Tech.*, vol. 6, no. 11, pp. 2989–3034, 2013, doi: 10.5194/amt-6-2989-2013.
[34] G. Huang, C. Huang, Z. Li, and H. Chen, "Development and validation of a robust algorithm for retrieving aerosol optical depth over land from MODIS data," *IEEE J. Sel. Topics Appl. Earth Obs. Remote Sens.*, vol. 8, no. 3, pp. 1152–1166, Mar. 2015.
[35] M. Bilal, J. E. Nichol, and M. Nazeer, "Validation of Aqua-MODIS C051 and C006 operational aerosol products using AERONET measurements over Pakistan," *IEEE J. Sel. Topics Appl. Earth Obs. Remote Sens.*, vol. 9, no. 5, pp. 2074–2080, May 2016.
[36] A. Huete, K. Didan, W. van Leeuwen, T. Miura, and E. Glenn, "MODIS vegetation indices," in *Land Remote Sensing and Global Environmental Change*, vol. 1. New York, NY, USA: Springer, 2011, pp. 579–602.
[37] E. F. Vermote and S. Y. Kotchenova. (2008). MOD09 user's Guide (J/OL). [Online]. Available: http://modis-sr.ltdri.org
[38] R. C. Levy, L. A. Remer, D. Tanré, S. Mattoo, and Y. J. Kaufman, "Algorithm for remote sensing of tropospheric aerosol over dark targets from MODIS: Collections 005 and 051: Collections 005 and 051: Revision 2; Feb. 2009," *MODIS Algorithm Theoretical Basis Document*, 2009b.
[39] Z. T. Wang *et al.*, "HJ-1 terrestrial aerosol data retrieval using deep blue algorithm," *J. Remote Sens.*, vol. 16, no. 3, pp. 596–610, 2012.
[40] J. He, Y. Zha, J. Zhang, J. Gao, Y. Li, and X. Chen, "Retrieval of aerosol optical thickness from HJ-1 CCD data based on MODIS-derived surface reflectance," *Int. J. Remote Sens.*, vol. 36, no. 3, pp. 882–898, 2015.
[41] E. F. Vermote, D. Tanré, J. L. Deuze, M. Herman, J. J. Morcrette, and S. Y. Kotchenova, *Second Simulation of a Satellite Signal in the Solar Spectrum-Vector (6SV), 6S User Guide Version 3*. New York, NY, USA: Wiley, 2006.
[42] B. N. Chew *et al.*, "Tropical cirrus cloud contamination in sun photometer data," *Atmos. Environ.*, vol. 45, no. 37, pp. 6724–6731, 2011.
[43] T. F. Eck *et al.*, "Wavelength dependence of the optical depth of biomass burning, urban, and desert dust aerosols," *J. Geophys. Res.*, vol. 104, no. D24, pp. 31333–31349, 1999.
[44] A. Ångström, "The parameters of atmospheric turbidity," *Tellus*, vol. 16, no. 1, pp. 64–75, 1964.
[45] Z. Li *et al.*, "Validation and understanding of moderate resolution imaging spectroradiometer aerosol products (C5) using ground-based measurements from the handheld Sun photometer network in China," *J. Geophys. Res.*, vol. 112, no. D22, pp. 365–371, 2007.
[46] D. A. Chu, Y. J. Kaufman, C. Ichoku, L. A. Remer, D. Tanré, and B. N. Holben, "Validation of MODIS aerosol optical depth retrieval over land," *Geophys. Res. Lett.*, vol. 29, no. 12, pp. MOD2-1–MOD2-4, 2002.
[47] Z. Li *et al.*, "Validation and understanding of moderate resolution imaging spectroradiometer aerosol products (C5) using ground-based measurements from the handheld sun photometer network in China," *J. Geophys. Res.*, vol. 112, no. D22, pp. 1–16, 2007.
[48] Q. He, C. Li, X. Tang, H. Li, F. Geng, and Y. Wu, "Validation of MODIS derived aerosol optical depth over the Yangtze River Delta in China," *Remote Sens. Environ.*, vol. 114, no. 8, pp. 1649–1661, 2010.

Jing Wei was born in Zibo, Shandong, China, in 1991. He received the B.E. degree in remote sensing science and technology in 2014 and will receive the M.E. degree in photogrammetry and remote sensing in 2017 from Geomatics College, Shandong University of Science and Technology, Qingdao, China.

His research interests focus on the high-resolution retrieval of aerosol optical depth from local and regional scales from multitype satellites images and cloud, cloud-shadow detection.

Lin Sun was born in Zaozhuang, Shandong, China, in 1975. He received the Ph.D. degree in cartography and geographical information system from the Institute of Remote Sensing and Digital Earth, Chinese Academy of Science, Beijing, China, in 2006.

From 2012 to 2014, he was a Visiting Scholar with the University of Maryland, USA. He is currently a Professor with Shandong University of Science and Technology, Qingdao, China. His main research interests include cloud detection and aerosol optical depth retrieval from satellite images. He is the gainer of "Excellent Young Scholars of the Nature Science Foundation of Shandong Province in China.